

On the stability of the satellites of asteroid 87 Sylvia

O. C. Winter,^{1*} L. A. G. Boldrin,¹ E. Vieira Neto,¹ R. Vieira Martins,²
S. M. Giuliatti Winter,¹ R. S. Gomes,² F. Marchis³ and P. Descamps⁴

¹São Paulo State University – UNESP, Grupo de Dinâmica Orbital & Planetologia, Guaratinguetá, CEP 12.516-410, Brazil

²Observatório Nacional, Rua General José Cristino, 77, CEP 20921-400, Rio de Janeiro, Brazil

³University of California at Berkeley, Department of Astronomy, 601 Campbell Hall, Berkeley, CA 94720, USA

⁴Institut de Mécanique Céleste et de Calcul des Éphémérides, Observatoire de Paris, 75014 Paris, France

Accepted 2009 January 26. Received 2009 January 14; in original form 2008 October 14

ABSTRACT

The triple asteroidal system (87) Sylvia is composed of a 280-km primary and two small moonlets named Romulus and Remus (Marchis et al. 2005b). Sylvia is located in the main asteroid belt, with semi-major axis of about 3.49 au, eccentricity of 0.08 and 11° of orbital inclination. The satellites are in nearly equatorial circular orbits around the primary, with orbital radius of about 1360 km (Romulus) and 710 km (Remus). In this work, we study the stability of the satellites Romulus and Remus. In order to identify the effects and the contribution of each perturber, we performed numerical simulations considering a set of different systems. The results from the three-body problem, Sylvia–Romulus–Remus, show no significant variation of their orbital elements. However, the inclinations of the satellites present a long-period evolution with amplitude of about 20° when the Sun is included in the system. Such amplitude is amplified to more than 50° when Jupiter is included. These evolutions are very similar for both satellites. An analysis of these results shows that Romulus and Remus are librating in a secular resonance and their longitude of the nodes are locked to each other. Further simulations show that the amplitude of oscillation of the satellites' inclination can reach higher values depending on the initial values of their longitude of pericentre. In those cases, the satellites get caught in an evection resonance with Jupiter, their eccentricities grow and they eventually collide with Sylvia. However, the orbital evolutions of the satellites became completely stable when the oblateness of Sylvia is included in the simulations. The value of Sylvia's J_2 is about 0.17, which is very high. However, even just 0.1 per cent of this value is enough to keep the satellite's orbital elements with no significant variation.

Key words: celestial mechanics – minor planets, asteroids.

1 INTRODUCTION

The first triple asteroidal system discovered was (87) Sylvia (Marchis et al. 2005b). The primary body is about 280 km, while the two small satellites, Romulus and Remus, are about 18 ± 4 and 7 ± 2 km, respectively. For simplicity, in this paper we will call the primary of the system (87) Sylvia as 'Sylvia'. The satellites are in nearly equatorial circular orbits around the primary, with orbital radius of about 1360 km (Romulus) and 710 km (Remus). In this paper, we study the stability of the satellites Romulus and Remus. Sylvia is located in the main asteroid belt, with semimajor axis of about 3.49 au, eccentricity of 0.08 and 11° of orbital inclination.

Therefore, the two main perturbers of the system are the Sun and Jupiter.

In order to identify the effects and the contributions of each relevant perturber of the system, we explored several different dynamical systems. We studied the interactions between the two satellites, the perturbation due to the Sun and due to the planet Jupiter. We identify two secular resonances that play important roles on the dynamics of such systems. Finally, we investigate the contribution due to the oblateness of Sylvia.

This paper has the following structure. In the next section, we present our numerical simulations considering different dynamical systems, the three-, four- and five-body problems. The effects due to the interaction between Romulus and Remus are analysed in Section 3. The occurrence of the evection resonance between the satellites and Jupiter and its consequences are shown in Section 4.

*E-mail: ocwinter@pq.cnpq.br

Section 5 is devoted to the effect of the oblateness; and finally, in Section 6, we present our conclusions.

2 SIMULATIONS OF THE THREE-, FOUR- AND FIVE-BODY PROBLEMS

We performed numerical simulations of several different dynamical systems. In all cases, we used the Gauss-Radau integrator (Everhart 1985) and considered a time-span of 5×10^4 years that corresponds to about 5×10^6 orbital periods of Romulus. Such time-span was found to be suitable in order to capture all the main long-term effects associated with the secular perturbations due to Jupiter. In order to check the accuracy of the numerical integrations, we

monitored the total energy of the system. The relative error was always lower than 10^{-11} . The physical and orbital data of the system (87) Sylvania adopted in most of the simulations are given in Table 1.

First of all, we looked at the orbital evolution of Sylvania. Sylvania's orbit around the Sun, under Jupiter's perturbation, presents a very stable evolution (Fig. 1). Its semimajor axis has only short-period oscillations with small amplitudes, while the eccentricity and inclination show periodic secular evolution with amplitudes of $\Delta e \simeq 0.1$ and $\Delta I \simeq 3^\circ$. This is the expected evolution due to the secular perturbation caused by Jupiter. Also in Fig. 1 (in red) the evolution of Sylvania's orbital elements under Jupiter's perturbation is shown, considering only the secular terms of the

Table 1. Physical and orbital data of Sylvania's system (Marchis et al. 2005b).

	Mass (kg)	a	e	I ($^\circ$)	Ω ($^\circ$)	w ($^\circ$)	f ($^\circ$)	Orbital period
Sylvia	1.4780×10^{19}	3.49 au	0.08	10.855	266,195	73,342	8,51412	6.52 yr
Romulus	3.6625×10^{15}	1356 km	0.001	1.7	273	101	81.88	3.65 d
Remus	2.1540×10^{14}	706 km	0.016	2.0	314	97	12.695	1.38 d

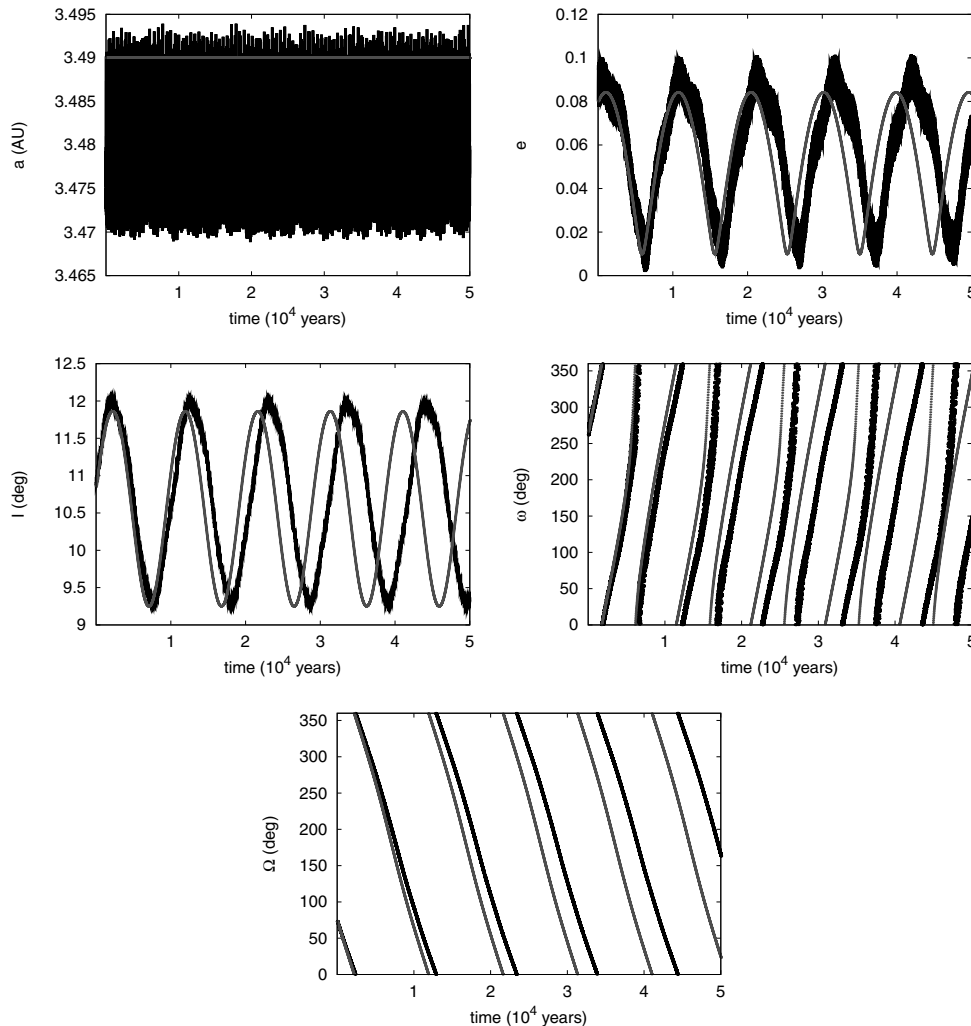


Figure 1. Temporal evolution of the semimajor axis, eccentricity, inclination, argument of pericentre and longitude of the ascending node of Sylvania. These are the results from the numerical integration of the five-body problem, Sylvania–Romulus–Remus–Sun–Jupiter, (in black) and from the secular perturbation theory, Sylvania–Sun–Jupiter (in red).

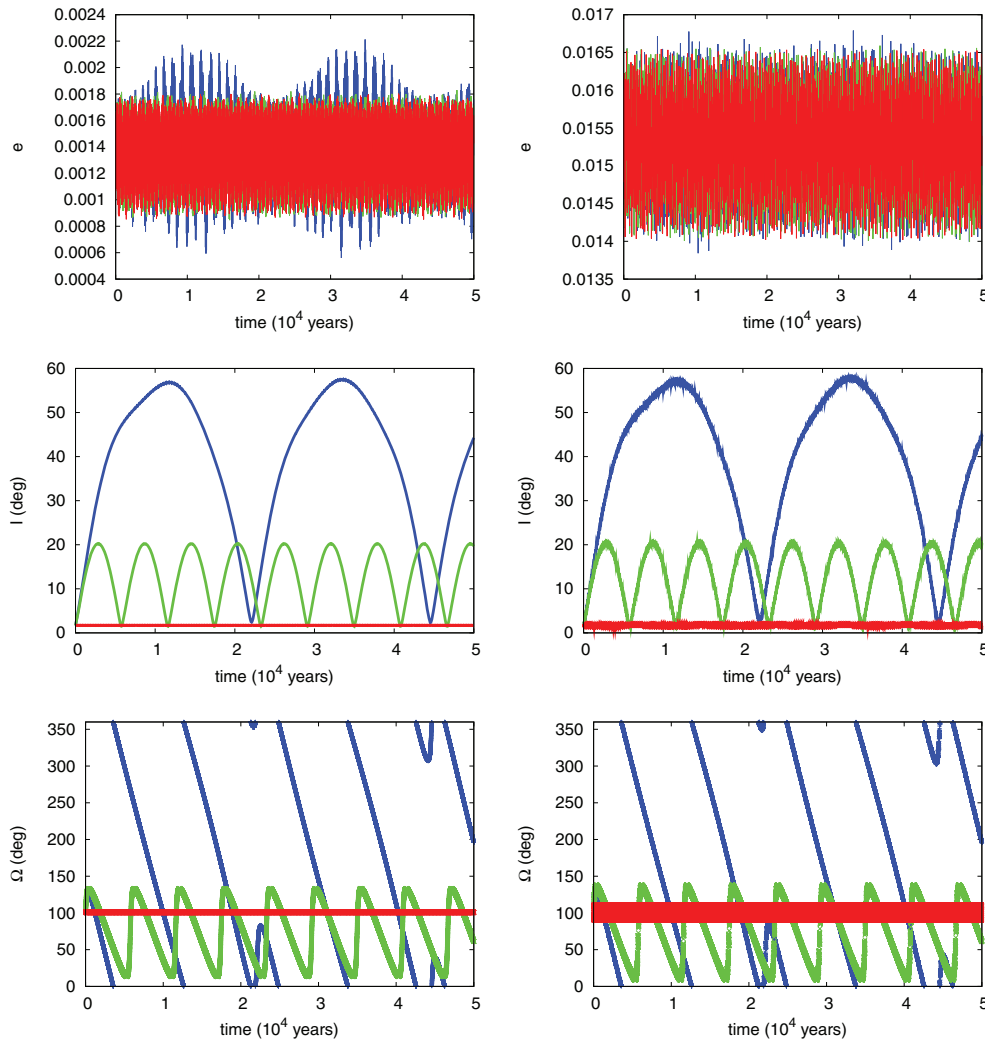


Figure 2. Temporal evolution of the eccentricity, the inclination and the longitude of the ascending node of Romulus (left-hand column) and Remus (right-hand column). In each frame, the results from three different numerical integrations are plotted. (1) In red, the three-body problem – Sylvia–Romulus–Remus. (2) In green, the four-body problem – Sylvia–Romulus–Remus–Sun. (3) In blue, the five-body problem – Sylvia–Romulus–Remus–Sun–Jupiter.

three-body disturbing function (chapter 7 of Murray & Dermott 1999).

Now we present the results of the numerical integrations for a set of different dynamical systems. Fig. 2 shows the temporal evolution of the eccentricity (e), the inclination (i) and the longitude of the ascending node (Ω) of Romulus (left-hand column) and Remus (right-hand column). In each frame of Fig. 2, the results from three different systems are plotted: the three-body problem, Sylvia–Romulus–Remus (in red); the four-body problem, Sylvia–Romulus–Remus–Sun (in green) and the five-body problem, Sylvia–Romulus–Remus–Sun–Jupiter (in blue).

The results from the three-body problem simulation, Sylvia–Romulus–Remus, show no significant variation of the satellite’s orbital elements. The inclusions of the Sun and Jupiter do not affect the evolution of the eccentricities of the satellites. However, their orbital inclinations show a significant change. They present a periodic secular evolution, having amplitude of about 20° with period of almost 6×10^3 years (only the Sun), and amplitude of about 58° with period of almost 22×10^3 years (Sun and Jupiter). Their longitudes of the node either librate with amplitude of more than 120° (only the Sun) or circulate (Sun + Jupiter).

We also note that the evolution of i and Ω for both satellites presents very similar amplitudes and frequencies. Of course, these evolutions are mainly due to the perturbations of the Sun (green) and Sun and Jupiter (blue), respectively. However, the fact of them being so similar is associated with a connection between Romulus and Remus, which will be discussed in the following section.

3 THE ROMULUS–REMUS CONNECTION

The gravitational interaction between Romulus and Remus produces different outcomes according to the dynamical system considered. In this section, we concentrate the analysis on the temporal evolution of the satellites’ orbital inclinations. We compare the results from our numerical integrations with results from the secular perturbation theory (see for instance Murray & Dermott 1999).

From the numerical integrations of the three-body system, Sylvia–Romulus–Remus (Fig. 2, in red), we see that Romulus produces oscillations of small amplitude ($<4^\circ$) on Remus’s inclination, which in return produces an even smaller amplitude of oscillation on Romulus’s inclination ($<1^\circ$). These results are very close to those obtained from the secular perturbation theory (Fig. 3, first row). The

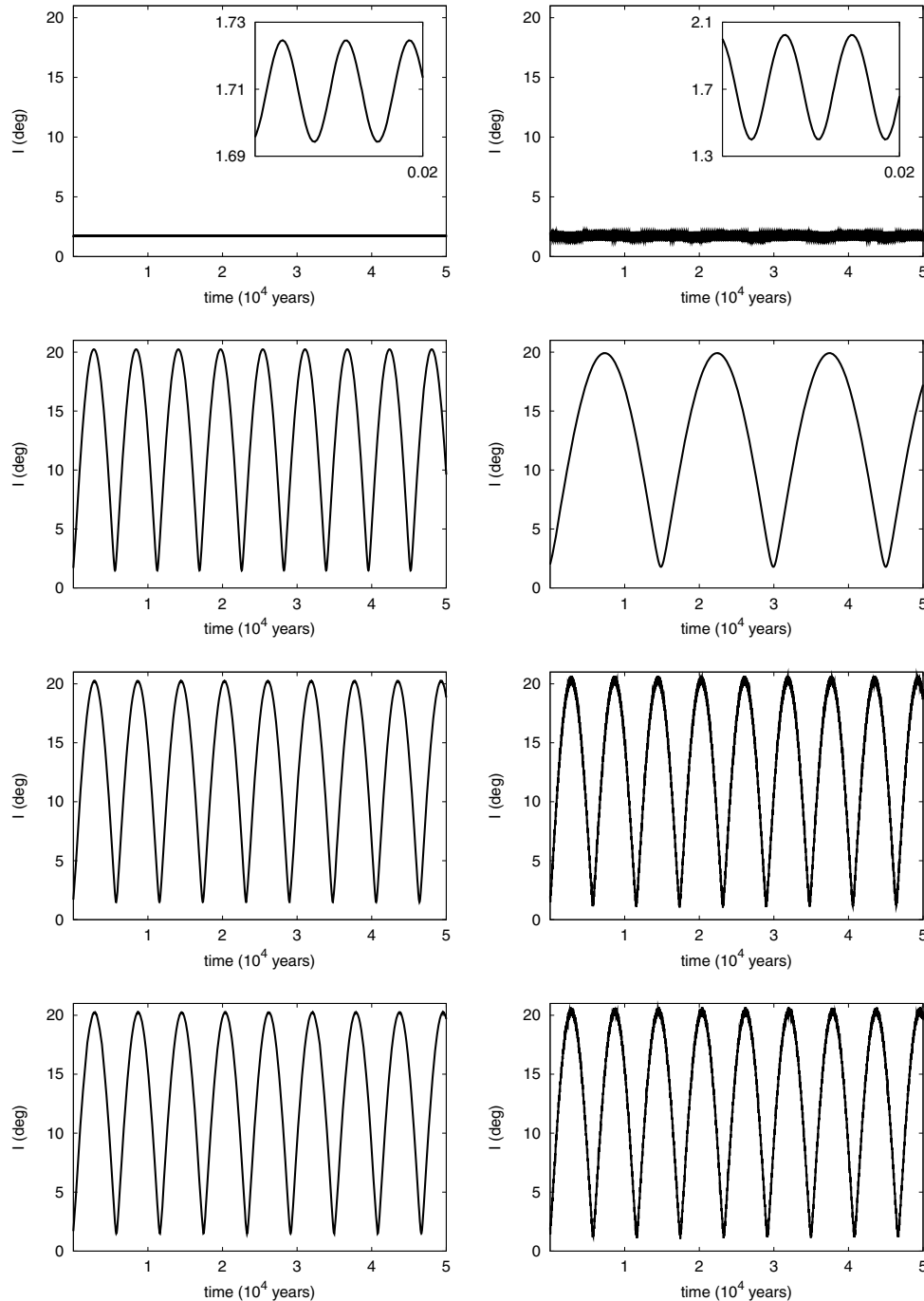


Figure 3. Temporal evolution of the orbital inclinations of Romulus (left-hand column) and Remus (right-hand column). In the first row, the results from the secular perturbation theory for the three-body system, Sylvia–Romulus–Remus, are presented. Also, a zoom of the plots is shown in the top-right corner of the respective figure. In the second row, the results from the secular perturbation theory for the three-body systems: Sylvia–Romulus–Sun (left-hand plot) and Sylvia–Remus–Sun (right-hand plot). In the third row, the results from the secular perturbation theory for the four-body system, Sylvia–Romulus–Remus–Sun, are presented. In the last row, the results from the numerical integration for the four-body system, Sylvia–Romulus–Remus–Sun, are presented (reproduced from Fig. 2, in green).

direct coupling between Romulus and Remus, showing that when the inclination of one increases the other decreases, is clearly seen in the zoom of these plots (Fig. 3, first row).

The secular perturbation from the Sun on Romulus and on Remus, separately, produces oscillations with the same amplitude ($\sim 20^\circ$), but with different periods (Fig. 3, second row). The period of oscillation for the inclination of Remus is more than twice than that

for Romulus. However, when the secular perturbation from the Sun and one of the satellites on the other satellite are computed, the amplitude and also the period of the oscillation of the inclination of both satellites are almost the same (Fig. 3, third row). Actually, the gravitational interaction between Romulus and Remus is such that Remus’s inclination very closely follows the behaviour of Romulus’s inclination. Such results are in very good agreement

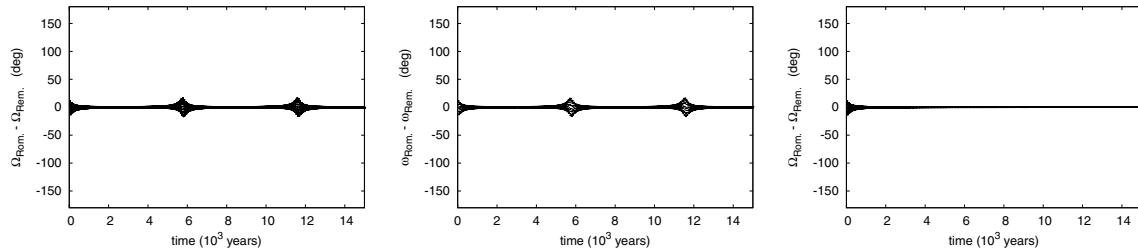


Figure 4. Temporal evolution of the resonant angle, given by the difference between the longitudes of the ascending nodes of Romulus and Remus, $\phi = \Omega_{\text{Rom}} - \Omega_{\text{Rem}}$. The left-hand plot is the result from the secular perturbation theory for the four-body system – Sylvia–Romulus–Remus–Sun. The central plot is the result from the numerical integration for the four-body problem – Sylvia–Romulus–Remus–Sun. The right-hand plot is the result from the numerical integration for the five-body problem – Sylvia–Romulus–Remus–Sun–Jupiter.

with our numerical integrations of the four-body problem – Sylvia–Romulus–Remus–Sun (Fig. 3, last row).

This connection between Romulus and Remus is due to a secular resonance. The longitude of the ascending node of both satellites is librating (Fig. 2, last row, in green). The evolution of the resonant angle, given by $\phi = \Omega_{\text{Rom}} - \Omega_{\text{Rem}}$, shows a libration of very short amplitude (Fig. 4, middle plot), i.e. the satellites’ longitudes of the ascending nodes get locked and librate with almost the same frequency, $\dot{\Omega}_{\text{Rom}} \approx \dot{\Omega}_{\text{Rem}}$. This result is also verified by the results from the secular perturbation theory (Fig. 4, left-hand plot).

Despite the fact that in the five-body problem, Sylvia–Romulus–Remus–Sun–Jupiter, the longitude of the ascending node of both satellites is circulating (Fig. 2, last row, in blue) that same secular resonance occurs (Fig. 4, right-hand plot). Therefore, the evolutions of the orbital inclination and longitude of the node of the two satellites are very much similar in the five-body system due to this secular resonance. If the gravitational influence of one of the satellites is not taken into account, their orbital evolutions are very different from each other (Fig. 5). The amplitude of Remus’s inclination is smaller than that of Romulus, and their eccentricities grow erratically. So, we conclude that the direct gravitational perturbation of one satellite on the other does not produce any significant variation on their orbital elements. However, when these satellites are under strong perturbations from the Sun and Jupiter, the two satellites get locked in a secular resonance such that the orbital evolution of one is very similar to the other.

4 THE EVECTION RESONANCE AND COLLISION

The amplitude of oscillation of the satellites’ inclinations can reach higher values depending on the initial value of Jupiter’s longitude of pericentre. In Fig. 6, we present the temporal evolution of the eccentricity and inclination of Romulus (left-hand column) and Remus (right-hand column), considering different initial values of Jupiter’s longitude of the pericentre. These are the results from the numerical integrations for the five-body system, Sylvia–Romulus–Remus–Sun–Jupiter, for $\varpi_{\text{Jup}} = 315^\circ$ (black), $\varpi_{\text{Jup}} = 320^\circ$ (green), $\varpi_{\text{Jup}} = 10^\circ$ (red) and $\varpi_{\text{Jup}} = 15^\circ$ (blue). We verified that for $-40^\circ \leq \varpi_{\text{Jup}} \leq 15^\circ$ the inclinations increase to higher values and the eccentricities suddenly grow until the satellites collide with Sylvia.

In those cases, the satellites get caught in an evection resonance with Jupiter. The evection resonance usually occurs when the period of the longitude of the pericentre of the satellite is very close to the orbital period of the perturber (Brouwer & Clemence 1961; Vieira Neto, Winter & Yokoyama 2006; Yokoyama et al. 2008). In this study, the resonant angle is given by the difference between the

satellite’s longitude of the pericentre and the mean longitude of Jupiter. In the first row of Fig. 7, an example of the evolutions of the evection angles of Romulus and Remus is presented for the case of initial $\varpi_{\text{Jup}} = 90^\circ$. One can note that when the evection angle starts to librate the corresponding eccentricity starts to grow until it reaches a collision with Sylvia.

5 OBLATENESS

In this section, the considered subject is the oblateness of Sylvia. First, we discuss the limitations of the shape determination of Sylvia from the observational images. Then, from secular perturbation theory (Ferraz-Mello 1979), we analyse the contribution of the Sun in comparison to that of Sylvia’s oblateness on the satellite’s orbital inclination. Finally, we present our numerical simulations for the five-body system, Sylvia–Romulus–Remus–Sun–Jupiter, including the oblateness of Sylvia.

5.1 Observational constraints

The J_2 of Sylvia was first measured from the analysis of both satellite orbits by Marchis et al. (2005b). The knowledge for each of them of its mean motion and semimajor axis constrains simultaneously both the mass of Sylvia and its J_2 through the generalized Kepler’s third law. The J_2 measured was thereby derived to be 0.175 ± 0.050 . The global shape of Sylvia was inferred from a convex inversion method of available light curves by Kaasalainen, Torppa & Piironen (2002). Furthermore, Marchis et al. (2006) recorded with the Keck Adaptive Optics system a resolved image of Sylvia’s primary at an angular resolution of 57 mas which agreed very well with this three-dimensional shape model validating the convex model. Using the three-dimensional shape model and assuming an uniform mass distribution in the interior of the primary, we calculate a theoretical J_2 of 0.12, globally consistent with the measured value although slightly lower. The discrepancy may arise either from an interior heterogeneity or from the shape model itself which could have some local non-convexities, not taken into account in the inversion process, able to further increase the J_2 of Sylvia.

5.2 Dynamical effect

In this section, we consider the effect of Sylvia’s oblateness (J_2) on the dynamics of Sylvia’s satellites. We define $\Pi = I \exp i\Omega$ as a complex variable associated with the inclination (I) and longitude of the ascending node (Ω). We use the indices ‘o’ for Romulus, ‘e’ for Remus and ‘S’ for the Sun. In what follows, we do not yet consider Sylvia’s oblateness. Thus the secular equation for a satellite’s Π

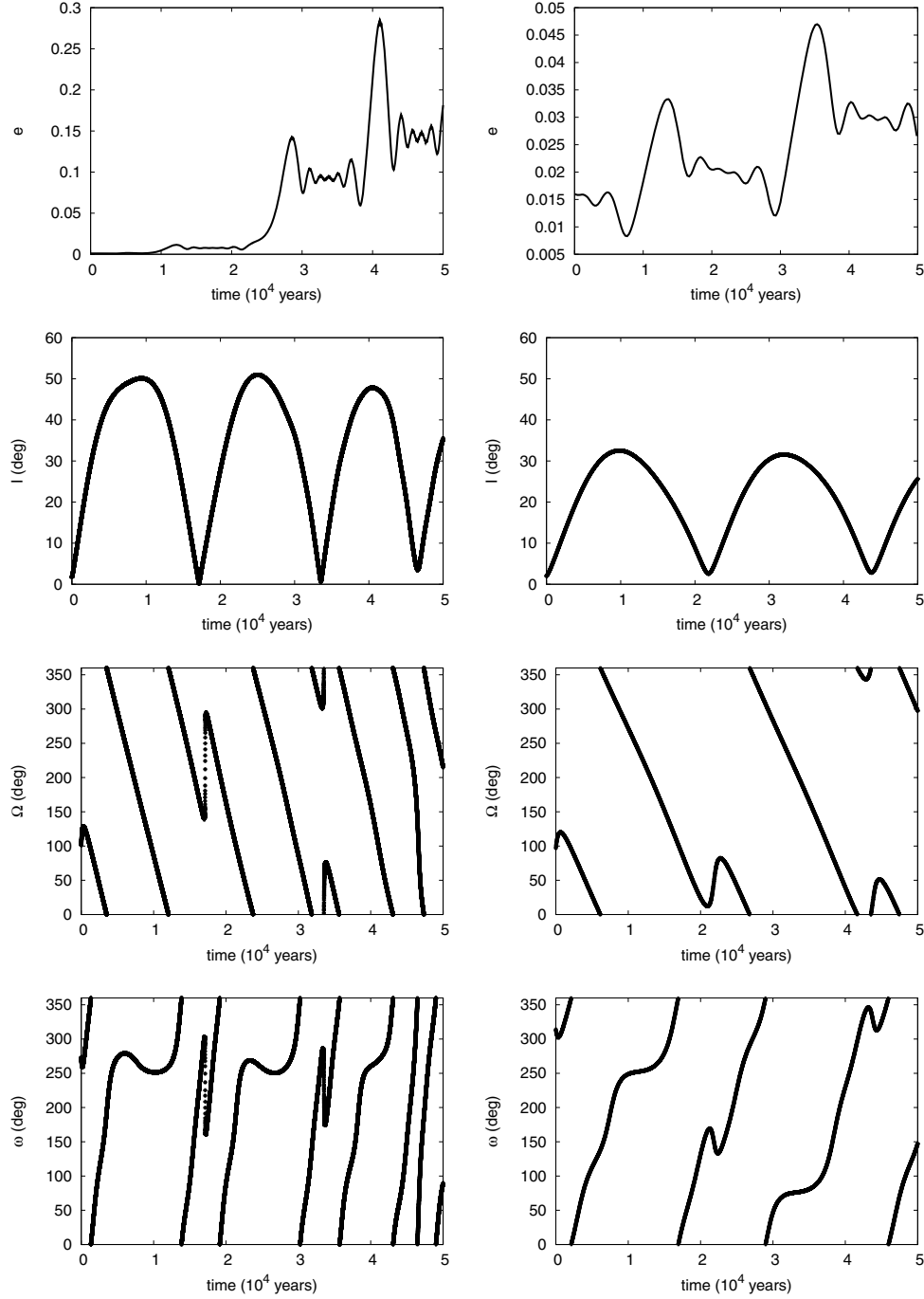


Figure 5. Temporal evolution of the eccentricity, inclination, longitude of the ascending node and argument of pericentre of Romulus (left-hand column) and Remus (right-hand column). These are the results from the numerical integrations for the four-body systems: Sylvia–Romulus–Sun–Jupiter (left-hand column) and Sylvia–Remus–Sun–Jupiter (right-hand column).

perturbed by the Sun is (Ferraz-Mello 1979)

$$\frac{d\Pi_o}{dt} = -iA_{S_o}\Pi_o + iA_{S_o}\Pi_S, \quad (1)$$

where

$$A_{S_o} = \frac{3Gm_S}{4n_o a_s^3}, \quad (2)$$

with an equivalent equation for Remus. Here, G is the gravitational constant, m is a mass, n a mean motion, a is a semimajor axis

and i is the imaginary unit. The solution of equation (1), in the approximation $\Pi_S = \text{constant}$, is

$$\Pi_o = K \exp ig_o t + \Pi_S, \quad (3)$$

where K is a complex constant and $g_o = -A_{S_o}$.

We obtain $A_{S_o} \sim 0.1108 \times 10^{-2} \text{ yr}^{-1}$, which corresponds to a period of 5673 years, confirming the results of Section 3. For Remus, we find a period of 15 012 years by the same method. The forced component Π_S induced by the Sun is thus responsible for

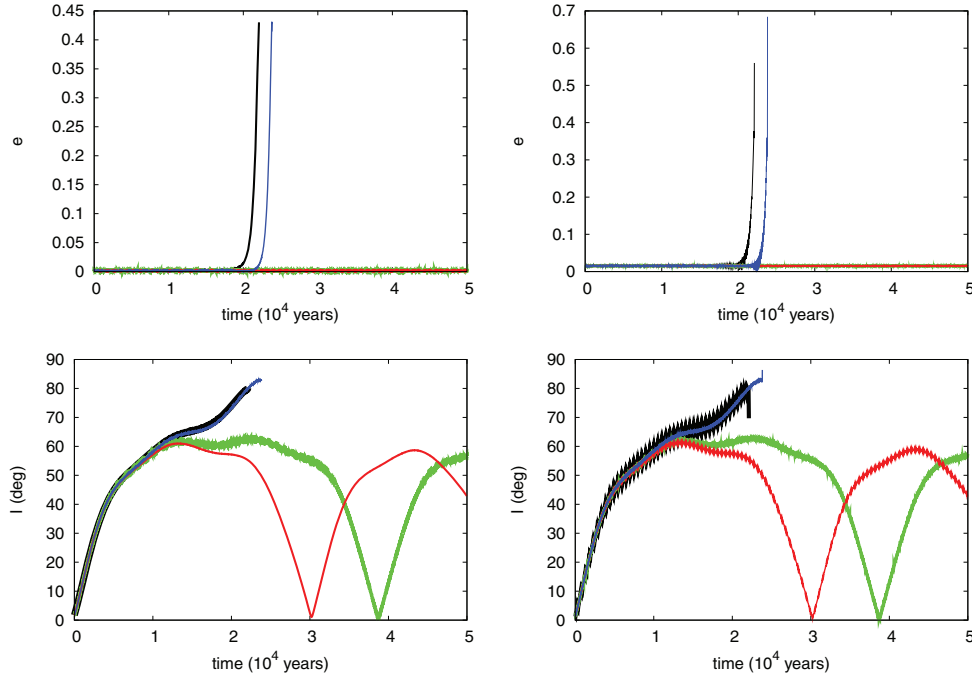


Figure 6. Temporal evolution of the eccentricity and inclination of Romulus (left-hand column) and Remus (right-hand column). These are the results from the numerical integrations for the five-body system Sylvia–Romulus–Remus–Sun–Jupiter, with different initial values of Jupiter’s longitude of the pericentre: $\varpi_{\text{Jup}} = 315^\circ$ (black); $\varpi_{\text{Jup}} = 320^\circ$ (green); $\varpi_{\text{Jup}} = 10^\circ$ (red); $\varpi_{\text{Jup}} = 15^\circ$ (blue).

the amplitude of the oscillation of I around 20° , since $|\Pi_S| \sim 10^\circ$ and the initial conditions for I_e and I_o are near 0° .

We now add the second satellite to the secular equations. To do this, we consider a complex vectorial variable $\mathbf{\Pi} = (\Pi_o, \Pi_e)$. The equation for the secular variation of $\mathbf{\Pi}$ (Ferraz-Mello 1979) is similar to equation (1):

$$\frac{d\Pi_o}{dt} = i\mathbf{A}\mathbf{\Pi} + i\mathbf{B}\Pi_S, \quad (4)$$

where \mathbf{A} is a 2×2 matrix with elements

$$A(1, 1) = -(A_e + A_{S_o}), \quad (5)$$

$$A(1, 2) = A_e, \quad (6)$$

$$A(2, 1) = A_o, \quad (7)$$

$$A(2, 2) = -(A_o + A_{S_e}), \quad (8)$$

and \mathbf{B} is a 2×1 vector with components

$$B(1) = A_{S_o}, \quad (9)$$

$$B(2) = A_{S_e}, \quad (10)$$

where

$$A_e = \frac{1}{4} \frac{Gm_e L}{n_o a_o^2}, \quad (11)$$

$$A_o = \frac{1}{4} \frac{Gm_o L}{n_e a_e^2}, \quad (12)$$

$$L = \frac{a_e}{a_o^2} b_{3/2}^{(1)}, \quad (13)$$

where $b_{3/2}^{(1)}$ is a Laplace coefficient (Ferraz-Mello 1979). The solution of equation (4) is quite similar to the one-dimensional case:

$$\mathbf{\Pi} = \mathbf{N}E + \mathbf{C}\Pi_S, \quad (14)$$

where \mathbf{N} is a 2×2 complex matrix whose rows are eigenvectors of matrix \mathbf{A} and the corresponding eigenvalues are g_1 and g_2 in $E = (\text{exp}ig_1, \text{exp}ig_2)$. \mathbf{C} is a ‘unitary’ vector (1, 1). This results from the fact that $A(j, 1) + A(j, 2) + B(j) = 0$ for $j = 1, 2$. As far as the forced component is concerned, both Romulus and Remus share a common one, given by the inclination of the Sylvia–Sun orbital plane with respect to Sylvia’s equator. Thus the 20° amplitude of oscillation of I_e and I_o is the same as in the case of just one satellite (Fig. 3). As to the frequencies of oscillation, they are the eigenfrequencies of matrix \mathbf{A} , and we find them to be

$$g_1 = -0.108 \times 10^{-2} \text{ yr}^{-1}, \quad (15)$$

$$g_2 = -0.832 \times 10^{-1} \text{ yr}^{-1}. \quad (16)$$

These correspond to periods of around 75 and 5820 years, a long period forced by the Sun and a short period due to the satellites themselves. This short period is similar to the secular one defined by just the two satellites around Sylvia, and the long period (similar to the period of Romulus in the Sylvia–Romulus–Sun problem) is shared by both satellites as shown in Fig. (3) (third and fourth row).

We now introduce the oblateness of Sylvia defined by its J_2 . To better understand its effect we first include it in the secular equations for just one satellite and the Sun. In this way, equation (1) becomes

$$\frac{d\Pi_o}{dt} = -i(A_{S_o} + A_{J_o}) + iA_{S_o}\Pi_S, \quad (17)$$

where

$$A_{J_o} = \frac{3}{2} \frac{GJ_2 m_{\text{sy}} b^2}{n_o a_o^5}. \quad (18)$$

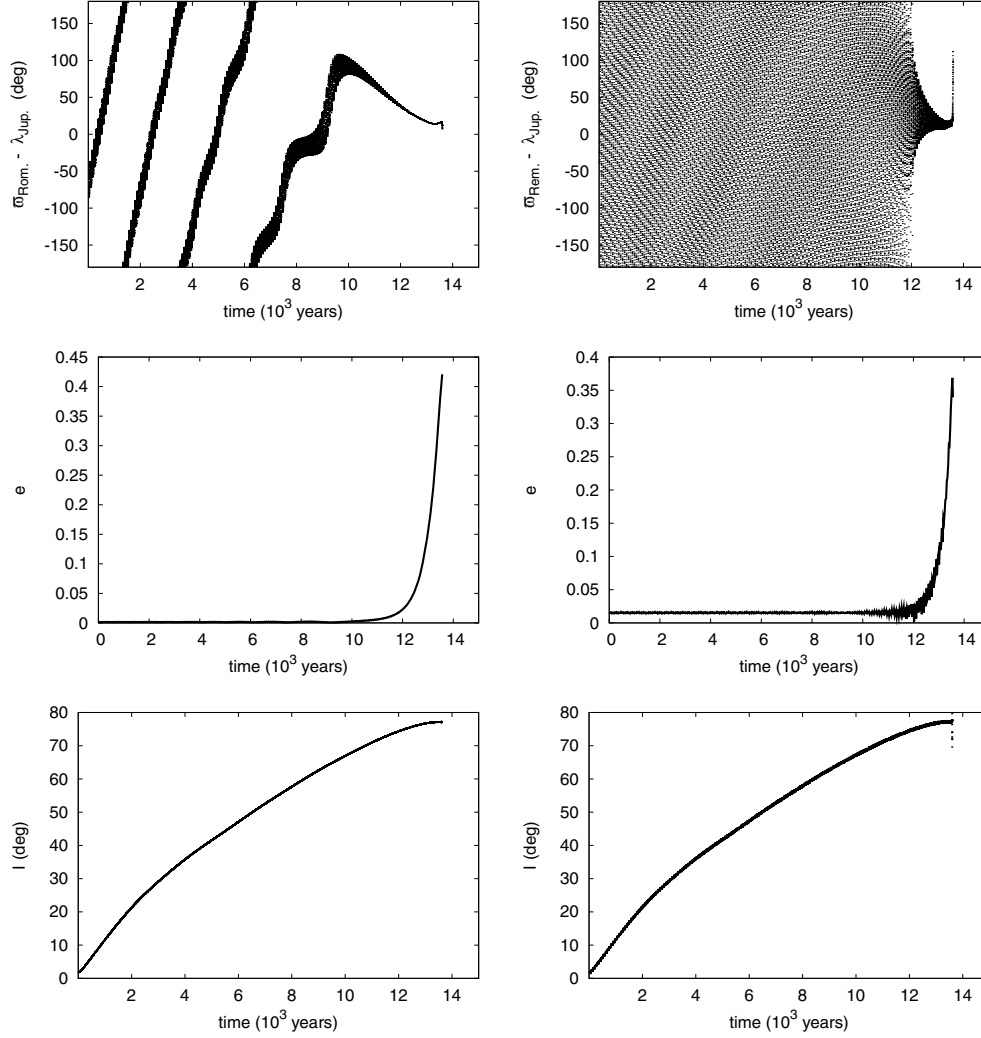


Figure 7. Temporal evolution of the evection angle, eccentricity and inclination of Romulus (left-hand column) and Remus (right-hand column). These are the results from the numerical integrations for the five-body system Sylvia–Romulus–Remus–Sun–Jupiter, with initial value of the satellite’s longitude of the pericentre equal to 90° .

Here, m_{sy} is Sylvia’s mass and b is Sylvia’s equatorial radius. Now the solution of (17) is

$$\Pi_o = K \exp i g_o t + c \Pi_S, \quad (19)$$

where K is a constant and

$$g_o = -(A_{S_o} + A_{J_o}), \quad (20)$$

$$c = \frac{A_{S_o}}{A_{S_o} + A_{J_o}}. \quad (21)$$

The value of A_{J_o} , with $J_2 = 0.17$, is 1.7401 yr^{-1} . Since $A_{J_o} \gg A_{S_o}$, first I_o will oscillate with a much higher frequency, and secondly the forced component, now multiplied by a very small constant c , will almost vanish.

The equations for both satellites, the Sun and including Sylvia’s oblateness, will be like equation (4), but the diagonal elements of matrix A are now

$$A(1, 1) = -(A_e + A_{S_o} + A_{J_o}), \quad (22)$$

$$A(2, 2) = -(A_o + A_{S_e} + A_{J_e}). \quad (23)$$

This will have important consequences on the eigenvalues (proper frequencies) and the forced components. They now become

$$g_1 = -1.745 \text{ yr}^{-1}, \quad (24)$$

$$g_2 = -17.04 \text{ yr}^{-1}, \quad (25)$$

$$C = (6.35 \times 10^{-4}, 2.75 \times 10^{-5}), \quad (26)$$

where $\mathbf{C} = \mathbf{A}^{-1}\mathbf{B}$. Thus the consequence of Sylvia’s oblateness is to critically stabilize the satellite’s orbits, since it introduces a frequency that is much faster than those generated by the other gravitational perturbations.

5.2.1 The effect of Jupiter

The direct effect of Jupiter on Sylvia’s satellites is negligible as compared with the Sun’s effect. However, by considering Jupiter, Sylvia’s orbital plane is no longer fixed but now precesses with a frequency given by

$$\mu = \frac{1}{4} \frac{G m_J L_J}{n_{\text{sy}} a_{\text{sy}}^2}, \quad (27)$$

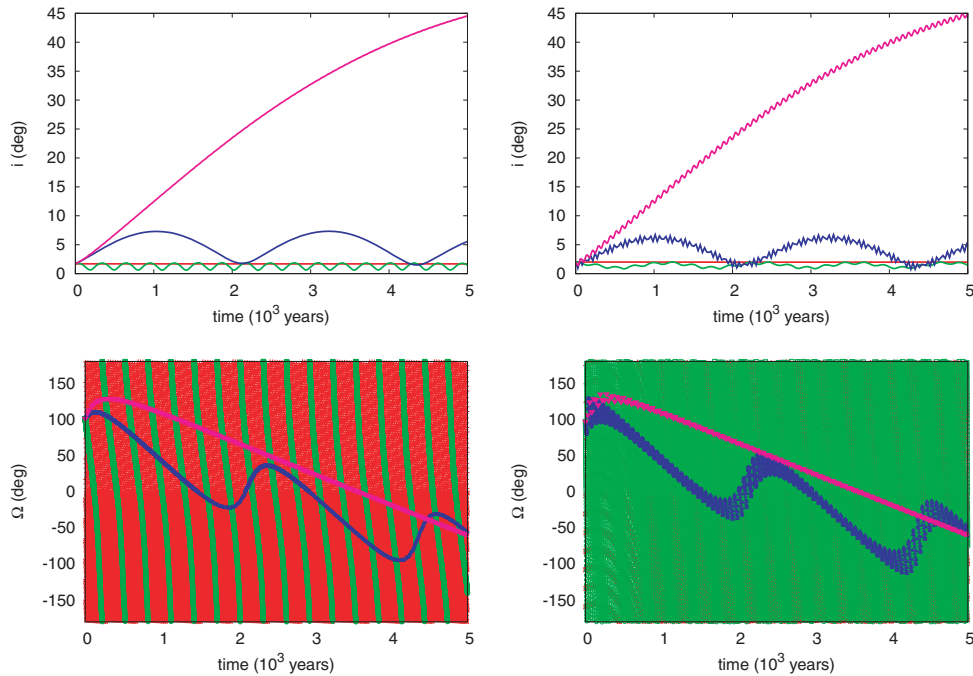


Figure 8. Temporal evolution of the inclination and the longitude of the ascending node of Romulus (left-hand column) and Remus (right-hand column). These are the results from the numerical integrations for the five-body system Sylvia–Romulus–Remus–Sun–Jupiter, with different values for J_2 of Sylvia. (i) In purple, $J_2 = 0$. (ii) In blue, $J_2 = 10^{-3} J_{2\text{Sylvia}}$. (iii) In green, $J_2 = 10^{-2} J_{2\text{Sylvia}}$. (iv) In red, $J_2 = J_{2\text{Sylvia}}$.

where the subscript ‘J’ refers to Jupiter and ‘Sy’ to Sylvia and

$$L_J = \frac{a_{\text{Sy}}}{a_J} b_{3/2}^{(1)}. \quad (28)$$

Since Jupiter has a non-zero inclination with respect to the reference plane (ecliptic) Sylvia’s inclination-node complex variable Π will be the sum of a constant forced component and a proper component precessing with frequency μ . Thus

$$\Pi_{\text{Sy}} = \Pi_J + K \exp -i\mu t, \quad (29)$$

where K is a constant to be determined as far as one knows Π_{Sy} for a specific time.

Now to solve equations (1), (4) and (17), we must replace the constant Π_S by Π_{Sy} given by equation (29). The solution for each equation and a specific satellite can be generally given by

$$\Pi_o = \Pi_{o_p} + k_1 K \exp -i\mu t + k_2 \Pi_J, \quad (30)$$

where Π_{o_p} is the proper component which will not change from the case without Jupiter, and

$$k_1 = \frac{A_{S_o}}{A_{S_o} + A_J - \mu} K, \quad (31)$$

$$k_2 = \frac{A_{S_o}}{A_{S_o} + A_J}, \quad (32)$$

for the case of just one satellite, here represented by Romulus (index ‘o’). When both satellites are included then k_1 and k_2 are two dimension vectors given by

$$k_1 = -(\mathbf{A} + \mu \mathbf{D})^{-1} \mathbf{B}, \quad (33)$$

$$k_2 = -\mathbf{A}^{-1} \mathbf{B}, \quad (34)$$

where \mathbf{A} and \mathbf{B} are matrices already defined for the case without Jupiter and ‘ \mathbf{D} ’ is the identity matrix.

This powerful effect of the oblateness was also explored in our numerical simulations. In Fig. 8, we present the results from the numerical integrations for the five-body system Sylvia–Romulus–Remus–Sun–Jupiter, with different values for J_2 of Sylvia: (i) in purple, $J_2 = 0$; (ii) in blue, $J_2 = 10^{-3} J_{2\text{Sylvia}}$; (iii) in green, $J_2 = 10^{-2} J_{2\text{Sylvia}}$; (iv) in red, $J_2 = J_{2\text{Sylvia}}$. The temporal evolution of the inclination and the longitude of the ascending node of Romulus (left-hand column) and Remus (right-hand column) clearly shows that the value of J_2 has to be much smaller (less than 1000 times) than the currently estimated value for Sylvia, in order to display any effect from other bodies’ perturbation.

6 CONCLUSIONS

We have explored the dynamics of the satellites of asteroid (87) Sylvia. When the oblateness of Sylvia is not taken into account, the satellites present a very interesting dynamical evolution. The perturbations from the Sun and Jupiter introduce a huge increase on the satellites orbital inclinations. Depending on the initial longitude of the pericentre of Jupiter, the satellites can be captured in a kind of evection resonance. The longitudes of pericentre of the satellites get locked to the mean longitude of Jupiter. Such resonance forces the satellites eccentricities to grow exponentially and they eventually collide with Sylvia. It is also noted that the evolutions of Romulus and Remus are very similar. This is due to a secular resonance between them, which is caused by the perturbations from the Sun and Jupiter. Finally, the complete stability of the satellites is guaranteed by the oblateness of Sylvia. We show that even just 1000 of the current value of J_2 would be enough to keep the satellites in stable orbits.

There are other triple asteroid systems in the main belt with similar characteristics, (45) Eugenia (Marchis et al. 2007) and (216) Kleopatra (Marchis et al. 2008), which will be studied by adopting a similar approach.

ACKNOWLEDGMENTS

This work was supported by the Brazilian agencies FAPESP, CNPq and CAPES. FM is supported by National Aeronautics and Space Administration issue through the Science Mission Directorate Research and Analysis programme no. NNX07AP70G.

REFERENCES

- Brouwer D., Clemence G. M., 1961, *Methods of Celestial Mechanics*. Academic Press, London
- Everhart E., 1985, in Carusi A., Valsecchi G., eds, *Dynamics of Comets: Their Origin and Evolution*. Dordrecht, Reidel, p. 185

- Ferraz-Mello S., 1979, *Dynamics of the Galilean Satellites: An Introductory Treatise*. Instituto Astronômico e Geofísico, Universidade de São Paulo, São Paulo
- Kaasalainen M., Torppa J., Piironen J., 2002, *Icarus*, 159, 369
- Marchis F., Descamps P., Hestroffer D., Berthier J., 2005a, *Nat*, 436, 822
- Marchis F., Descamps P., Hestroffer D., Berthier J., Brown M. E., Margot J.-L., 2005b, *IAU Circ.*, 8582
- Marchis F., Kaasalainen M., Hom E. F. Y., Berthier J., Enriquez J., Hestroffer D., Le Mignant D., de Pater I., 2006, *Icarus*, 185, 39
- Marchis F., Baek M., Descamps P., Berthier J., Hestroffer D., Vachier F., 2007, *IAU Circ.*, 8817
- Marchis F., Descamps P., Berthier J., Emery J. P., 2008, *IAU Circ. no. 8980*
- Murray C. D., Dermott S. F., 1999, *Solar System Dynamics*. Cambridge Univ. Press, Cambridge
- Vieira Neto E., Winter O. C., Yokoyama T., 2006, *A&A*, 452, 1091
- Yokoyama T., Vieira Neto E., Winter O. C., Sanches D. M., Brasil P. I., 2008, *Mathematical Problems in Engineering*, 2008, 251978

This paper has been typeset from a $\text{\TeX}/\text{\LaTeX}$ file prepared by the author.